

Equivalence Principles Based Skin Deformation of Character Animation

L. H. You¹, E. Chaudhry¹, X. Y. You², and Jian J. Zhang¹

National Centre for Computer Animation, Bournemouth University, United Kingdom

Faculty of Engineering and Computing, Coventry University, United Kingdom

Abstract – Based on the equivalence principles of physical properties, geometric properties and externally applied forces between a surface and the corresponding curves, we present a fast physics and example based skin deformation method for character animation in this paper. The main idea is to represent the skin surface and its deformations with a group of curves whose computation incurs much less computing overheads than the direct surface-based approach. The geometric and physical properties together with externally applied forces of the curves are determined from those of the surface defined by these curves according to the equivalence principles between the surface and the curves. This ensures the curve-based approach is equivalent to the original problem. A fourth order ordinary differential equation is introduced to describe the deformations of the curves between two example skin shapes which relates geometric and physical properties and externally applied forces to shape changes of the curves. The skin deformation is determined from these deformed curves. Several examples are given in this paper to demonstrate the application of the method.

Keywords: character animation, skin deformation, equivalence principles between surfaces and curves, physics and example based approach, fourth order ordinary differential equation

1. Introduction

In order to create realistic character animation, skin deformation has attracted a lot of research attention. Among various developed methods, three approaches have become the most popular. They are: joint-related, example-based and physics-based.

Since skin deformation is driven by the rotation of joints, joint-related approach controls the skin shape by the transformations associated with the joints of the skeleton. This approach is simple to use and fast to compute, and has been included in many animation packages. However, it suffers from some defects such as the collapsing joint and candy-wrapper effect.

Not relating skin deformation to the rotation of joints, the example-based approach generates high quality skinning with a limited number of example poses. Such an approach transforms the problem of skin deformation into that of shape interpolation. It does not require any manual skills to specify the weights required by joint-related approach and expensive calculation occurring in physics-based approach. One disadvantage of this approach is that sufficient example skin shapes must be known to achieve realistic skin deformation.

The realism of skin deformation can be improved by introducing the anatomy and biomechanics of skin deformation caused by the movements of muscles and tendons. The research activities in this field led to the development of physics-based approach. Such an approach

can create more realistic appearance of skin deformation, but requires more computation cost and computer resource.

This paper is an extended version of the work given in [1]. It aims at maximizing the strengths of the physics-based approach, example-based approach and curve-based surface modelling, but minimizing the weakness of physics and example based techniques. It uses surface curves to define the skin shape, determines the physical properties, geometric properties and externally applied forces of the surface curves through investigating the equivalence principles between a surface and the corresponding curves, and describes the shape changes for reducing computational cost. We introduce the underlying physical law of curve deformations for the interpolation of shape examples. In comparison with existing example-based approach, we need a smaller number of skin shapes and still manage to improve the realism of skin deformation.

2. Related work

Joint-related skin deformation was first investigated by Thalmann et al [2]. Later on, Lander described the basic principles of skeleton subspace deformation [3,4]. Weber discovered the shrinkage problem around a joint, around which bending or twisting occurs [5]. One remedy was the multi-weight enveloping technique proposed by Wang and Phillips [6]. Mohr and Gleicher added additional joints [7]. Kavan and Šára presented the spherical blend skinning [8]. Yang et al. proposed curve skeleton skinning [9].

In addition to joint-related skin deformation, example-based skin deformation was also proposed. Lewis et al.

*Corresponding author:
E-mail: lyou@bournemouth.ac.uk

developed the pose space deformation (PSD) technique which generalizes and improves both shape interpolation and common skeleton-driven deformation techniques [10]. Rhee et al. extended this approach to weighted pose-space deformation (WPSD) [11]. Mohr and Gleicher investigated an automated method to build character skins from a set of examples [12]. Allen et al. examined an example-based approach for determining skeleton-driven skin deformations [13]. Kurihara and Miyata developed a new method to construct an example-based deformable human hand model from CT scans [14]. Weber et al. proposed a system for skeletal shape deformation which operates based on given deformation examples [15].

In order to improve the realism of skin deformation, physics-based approaches were also introduced. Scheepers et al. considered the influence of the musculature on exterior form, developed anatomy-based models of muscles, and applied them to the torso and arm of a human figure [16]. Modelling muscles, bones, and generalized tissue as triangle meshes or ellipsoids, and treating muscles as deformable discretized cylinders, Jane and Allen proposed an improved, anatomically based approach [17]. Based on anatomy concepts, Nedel and Thalmann presented a method which represents a human model with three layers: skeleton, muscle and skin [18]. They introduced a mass-spring system with angular springs to physically simulate muscle deformations [19]. Aibel and Thalmann also proposed a muscle model based on physiological and anatomical considerations [20]. With a layered canonical model, Maryann et al. studied a semi-automatic technique for creating 3D models of creatures [21]. Using quasi-static linear deformation model and finite element method to calculate the deformation of chunks, Guo and Wong gave an approach to create skin deformations [22]. Venkataraman et al. introduced a combination of a kinematic and a variational model to deal with the wrinkling of skin [23]. Yang and Zhang presented a new anatomy-based skin deformation method [24]. You et al. investigated dynamic modelling of skin deformation [25].

Unlike the above methods where the deformation is based on the changes of surface shapes, some researchers used cross-section curves to describe character models because most of them have a cylinder-like topology. Shen and Thalmann used cross-sectional contours to represent skin surfaces and deform human limbs and torso by geometrically manipulating these cross-sectional contours [26]. Pyun et al. tried to extract wire curves and deformation parameters from a facial model [27]. Hyun et al. applied elliptic cross-sections to approximate various human body parts [28]. With the same elliptic cross-sections, Yoon et al. developed a sweep-based deformation [29]. Recently, Jha investigated how to construct branching surfaces from 2D contour curves [30].

The work introduced in this paper is to investigate the equivalence principles between a surface and the curves

defining the surface, and propose a physics and example based skin deformation model based on surface curves that define the skin. Through this model, the skin deformation is related to the geometric and physical properties as well as externally applied forces. How these geometric and physical properties and externally applied forces affect skin deformation is investigated and some examples are presented to demonstrate the applications of our proposed approach in skin deformation.

3. Using surface curves to describe and manipulate surfaces

The shape of a surface can be described by some curves on the surface. When the surface moves or deforms, these surface curves also change their shape. Due to this observation, we can animate the surface by animating these surface curves.

In order to use surface curves to animate a surface, we must find out the relationships between surface curves and the surface described by these curves. They include: how to obtain the surface curves describing a surface from a polygon model, and how to transfer the deformations of the surface curves to the polygon model. We will investigate these issues in this section.

3.1 Determination of surface curves from polygon models

Since manual determination of surface curves on a polygon model is time-consuming and tedious, we here introduce an automatic method.

For a polygon model shown in Figure 1a, we first draw a rough central line within the model. Then some points with an equal or unequal interval are located on the central line. From each point, we create a plane perpendicular to the central line, and use this plane to find out the intersecting points between the plane and the polygon model which form a surface curve on the polygon model. With such a treatment, we obtain all the surface curves of the polygon model as indicated in Figure 1b. It can be seen from the figure that some two adjacent surface curves may intersect. In order to avoid this, we rotate one of the two adjacent planes a little to

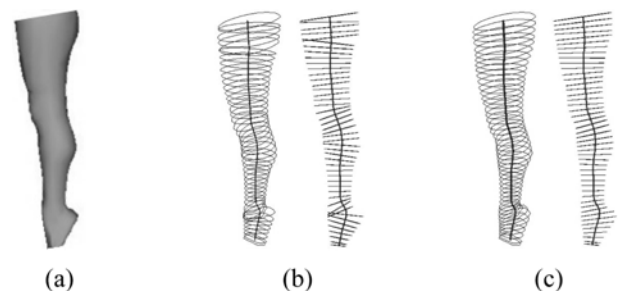


Fig. 1. Generation of surface curves. (a) Original model. (b) Surface curves with intersection. (c) Surface curves without intersection.

make the two adjacent surface curves not intersect. In this way, the surface curves in Figure 1b are changed into those in Figure 1c. Here the images on the left of Figures 1b and 1c are from the perspective view and those on the right of Figures 1b and 1c are from front view

3.2 Deformation transfer between surface curves and polygon models

After the surface curves describing a polygon model are obtained, we can deform these surface curves and transfer the deformations of these surface curves to the polygon model to achieve the new shape of the polygon model. Through this method, we can animate a polygon model by animating the surface curves describing the model.

There are two ways which can be used for this purpose. One is to create a new model from these surface curves through the skinning method, and the other is to relate all surface points of the polygon model to these surface curves. Here, we adopt the latter. The basic idea of doing this is to find the position of a surface point on a surface curve or between two adjacent surface curves and use this position to determine the displacement of the surface point.

For a surface point \mathbf{p}_o on one of the surface curves \mathbf{c}_1 as indicated in Figure 2a, we find two points \mathbf{p}_1 and \mathbf{p}_2 of the surface curve which are closest to the surface point \mathbf{p}_o . When the surface curve \mathbf{C}_1 is deformed into \mathbf{C}'_1 , the two curve points \mathbf{p}_1 and \mathbf{p}_2 are moved to \mathbf{p}'_1 and \mathbf{p}'_2 . The new position \mathbf{p}'_o of the surface point \mathbf{p}_o is determined by $\frac{\mathbf{p}'_1\mathbf{p}'_o}{\mathbf{p}'_1\mathbf{p}'_2} = \frac{\mathbf{p}_1\mathbf{p}_o}{\mathbf{p}_1\mathbf{p}_2}$.

For a surface point \mathbf{p}_o between two adjacent surface curves \mathbf{C}_1 and \mathbf{C}_2 as indicated in Figure 2b, we first calculate the geometric centre \mathbf{O}_1 of surface curve \mathbf{C}_1 and the geometric centre \mathbf{O}_2 of surface curve \mathbf{C}_2 . Then we generate a plane through points \mathbf{p}_o , \mathbf{O}_1 and \mathbf{O}_2 which intersects surface curves \mathbf{C}_1 and \mathbf{C}_1 . Among the intersection points between the plane and surface curve \mathbf{C}_1 , the one closest to point \mathbf{p}_o is taken to be \mathbf{p}_1 . Similarly, the point on surface curve \mathbf{C}_2 which is closet to point \mathbf{p}_o is taken to be \mathbf{p}_2 . Next, we determine the position of point \mathbf{p}_3 through the perpendicular relation between lines $\mathbf{p}_o\mathbf{p}_3$ and $\mathbf{p}_1\mathbf{p}_2$. Similarly, we obtain the position of point \mathbf{O}_3 through the perpendicular relation between lines $\mathbf{p}_o\mathbf{O}_3$ and $\mathbf{O}_1\mathbf{O}_2$.

After surface curves \mathbf{C}_1 and \mathbf{C}_2 are deformed into \mathbf{C}'_1 and \mathbf{C}'_2 , points \mathbf{p}_1 and \mathbf{p}_2 are moved to points \mathbf{p}'_1 and

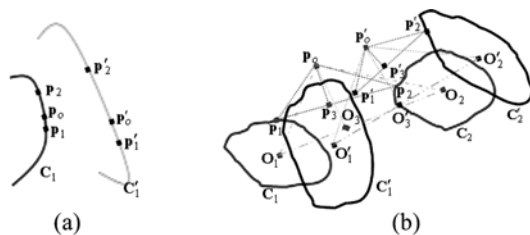


Fig. 2. Deformation transfer through surface curves and surface points.

\mathbf{p}'_2 , and the geometric centres \mathbf{O}_1 and \mathbf{O}_2 are moved to \mathbf{O}'_1 and \mathbf{O}'_2 , respectively. From points \mathbf{p}'_1 and \mathbf{p}'_2 , we can determine the new position \mathbf{p}'_3 of point \mathbf{p}_3 by the equation of $\frac{\mathbf{p}'_1\mathbf{p}'_3}{\mathbf{p}'_1\mathbf{p}'_2} = \frac{\mathbf{p}_1\mathbf{p}_3}{\mathbf{p}_1\mathbf{p}_2}$. From the geometric centres \mathbf{O}'_1 and \mathbf{O}'_2 , we can determine the new position \mathbf{O}'_3 of point \mathbf{O}_3 by the equation $\frac{\mathbf{O}'_1\mathbf{O}'_3}{\mathbf{O}'_1\mathbf{O}'_2} = \frac{\mathbf{O}_1\mathbf{O}_3}{\mathbf{O}_1\mathbf{O}_2}$. The new position \mathbf{p}'_o of point \mathbf{p}_o is determined by $\frac{\mathbf{p}'_o\mathbf{p}'_3}{\mathbf{p}'_o\mathbf{O}'_3} = \frac{\mathbf{p}_o\mathbf{p}_3}{\mathbf{p}_o\mathbf{O}_3}$.

4. Equivalence of surface curves and a surface

Surface deformations based on the underlying physical law have a potential to create a more realistic appearance of an object. To this aim, we discuss the equivalent methods of physical deformations between surface curves and the surface described by these curves.

When taking into account the physical and geometric properties, three factors affect the deformations. They are: physical properties, geometric properties and externally applied forces causing the deformations. If we can find proper physical and geometric properties as well as externally applied forces of the surface curves which can lead to the same deformation of the surface, the surface deformations will be transformed into those of the surface curves. Therefore, we will discuss how to determine physical properties, geometric properties and externally applied forces of surface curves defining a surface.

4.1 Physical properties of surface curves

According to the theory of solid mechanics, there are a number of different types of deformations, such as elastic deformation, plastic deformation, and buckling. Among them, elastic deformation represents the most common type of deformations. In this paper, we will only consider this type of deformation.

Besides the dependence of the physical properties on the types of deformations, they also depend on the different materials. In general, materials can be divided into three large classes: isotropic, orthotropic and anisotropic. Isotropic materials have the same physical properties in any directions. Orthotropic materials have the same physical properties in the same direction but different physical properties in the perpendicular direction. Anisotropic materials have different properties in different directions. Among them, isotropic materials are most frequently applied.

For the deformations of isotropic materials caused by sculpting forces, two physical properties: Young's modulus E and Poisson's ratio ν , are used to describe the relationship between them and deformations.

If the surface and the curves defining the surface are made of the same isotropic materials, Young's modulus and Poisson's ratio of surface curves are the same as those of the surface.

4.2 Geometric properties of surface curves

Now, we discuss how to determine the equivalent

geometric properties of curves. Since bending deformation of a curve is similar to that of an elastic beam subjected to bending loads, we can determine geometric properties of a surface curve using the method determining geometric properties of an elastic beam. Similarly, bending deformation of a surface is similar to that of an elastic plate. Due to this reason, the geometric properties of a surface for bending deformation can be determined with the similar method to that of an elastic plate subjected to the same deformation.

According to the theory of plate bending, the bending rigidity of unit width is $Eh^3/[12(1-\nu^2)]$ where h is the thickness of the plate. From the theory of beam bending, the bending rigidity of a beam with width b and height h is $Ebh^3/12$ where $bh^3/12$ is called the moment of inertia which is a geometric property of the beam.

If the thickness of a surface is h , and the width between two adjacent surface curves $i-1$ and i is b_{i-1} and that between two adjacent surface curves i and $i+1$ is b_i , the moment of inertia of surface curve i is $(b_{i-1} + b_i)h^3/[24(1-\nu^2)]$. If I is a boundary curve which situates at the boundary of a deformation region, and the width between curves I_{i-1} and I is b_{i-1} , the moment of inertia of surface curve I is $b_{i-1}h^3/[24(1-\nu^2)]$.

4.3 Equivalent forces of surface curves

In this subsection, we discuss how to transform the bending loads acting on a surface into those on the surface curves which are used to describe the surface using the principle of deformation equivalence. This principle states: the forces acting on a surface and those acting on the curves defining the surface should produce the same deformations.

According to Section 5 below, the mathematical model of curve deformation can be described with equation (13). For curve deformation with both positional and tangential continuities, the boundary constraints can be written as

$$\begin{aligned}
 v=0 \quad \mathbf{X}_i(v) &= 0 \quad \frac{\partial \mathbf{X}_i(v)}{\partial v} = 0 \\
 v=1 \quad \mathbf{X}_i(v) &= 0 \quad \frac{\partial \mathbf{X}_i(v)}{\partial v} = 0
 \end{aligned}
 \tag{1}$$

where v is a parametric variable, \mathbf{X} is a vector-valued deformation function which has three components x , y and z , and the subscript i indicates the i^{th} curve.

The externally applied force $\mathbf{P}_i(v)$ acting on the i^{th} curve has two different types: concentrated force and line distribution force. These two types of forces can be mathematically unified as

$$\mathbf{P}_i(v) = \sum_{n=1}^{\bar{N}} \mathbf{p}_{in} \sin n \pi v
 \tag{2}$$

where $\mathbf{p}_{in}(n = 1, 2, \dots, \bar{N})$ are unknown coefficients.

For a concentrated force \mathbf{p}_i acting at any position v_{p0} of curve i , the coefficients \mathbf{p}_{in} are determined by

$$\mathbf{p}_{in} = 2\mathbf{p}_i \sin n \pi v_{p0}
 \tag{3}$$

For a uniformly distributed line force \mathbf{p}_i acting within a range $\{v_{p0} \leq v \leq v_{p1}\}$, the coefficients \mathbf{p}_{in} are determined by

$$\mathbf{p}_{in} = 2\mathbf{p}_i / (n\pi) \sin n\pi(v_{p1} + v_{p0}) / 2 \sin n\pi(v_{p1} - v_{p0}) / 2
 \tag{4}$$

The solution of equation (13) corresponding to externally applied force (2) and boundary constraints (1) represents a deformation curve and can take the following form

$$X_i(v) = \sum_{i=0}^3 \mathbf{e}_i v^i + \sum_{n=1}^{\bar{N}} \mathbf{d}_{in} \sin n \pi v
 \tag{5}$$

where $\mathbf{e}_i(v)$ ($i = 0, 1, 2, 3$) are unknown constants, and \bar{N} is the number of terms in the sine series.

Substituting equation (5) into boundary conditions (1), solving for the unknown constants, inserting them back to equation (5), and making use of equation (13), we obtain

$$\begin{aligned}
 \mathbf{X}_i(v) &= \\
 &= \frac{1}{EI_i \pi^4} \sum_{n=1}^{\bar{N}} \frac{\mathbf{p}_{in}}{n^3} \left\{ \pi \{ -1 + [2 + (-1)^n]v - [1 + (-1)^n]v^2 \} v + \frac{1}{n} \sin n \pi v \right\}
 \end{aligned}
 \tag{6}$$

For surface manipulation, many situations are to change the shape of a surface within a local region. At the interface between the un-deformed region and deformed region, the surface should maintain smooth transition, i. e., no deformation and tangent changes occurs at the interface which can be described with the following equation

$$\begin{aligned}
 u=0 \quad X(u,v) &= 0 \quad \frac{\partial \mathbf{X}(u,v)}{\partial u} = 0 \\
 u=1 \quad X(u,v) &= 0 \quad \frac{\partial \mathbf{X}(u,v)}{\partial u} = 0 \\
 v=0 \quad X(u,v) &= 0 \quad \frac{\partial \mathbf{X}(u,v)}{\partial v} = 0 \\
 v=1 \quad X(u,v) &= 0 \quad \frac{\partial \mathbf{X}(u,v)}{\partial v} = 0
 \end{aligned}
 \tag{7}$$

where u and v are two parametric variables, and \mathbf{X} is a vector-valued deformation function.

Since the deformation of a surface is similar to that of

an elastic plate, the mathematical model of the surface deformation can be derived from that of bending deformation of an elastic plate which can be written as

$$EH^3/[12(1-\nu^2)]\left[\frac{\partial^4}{\partial u^4}+2\frac{\partial^4}{\partial u^2\partial v^2}+\frac{\partial^4}{\partial v^4}\right]\mathbf{X}(u,v)=\mathbf{P}(u,v) \tag{8}$$

where $\mathbf{P}(u,v)$ is an externally applied force.

Partial differential equation (8) can be solved with the finite difference method. Using the central difference algorithm given in [31] and the mesh shown in Figure 3, we change the fourth order partial difference equation into a finite difference equation below

$$20\mathbf{X}_0-8(\mathbf{X}_1+\mathbf{X}_2+\mathbf{X}_3+\mathbf{X}_4)+2(\mathbf{X}_5+\mathbf{X}_6+\mathbf{X}_7+\mathbf{X}_8) \\ (\mathbf{X}_9+\mathbf{X}_{10}+\mathbf{X}_{11}+\mathbf{X}_{12})=\frac{12(1-\nu)}{Eh^3}\delta^4\mathbf{P}_0 \tag{9}$$

where δ is the interval between two adjacent nodes.

Using the same central difference algorithm, boundary constraints can be changed into

$$\begin{aligned} u=0 \quad \mathbf{X}_0=0 \quad \mathbf{X}_1-\mathbf{X}_3=0 \\ u=1 \quad \bar{\mathbf{X}}_0=0 \quad \bar{\mathbf{X}}_1-\bar{\mathbf{X}}_3=0 \\ v=0 \quad \mathbf{X}_0=0 \quad \mathbf{X}_2-\mathbf{X}_4=0 \\ v=1 \quad \bar{\mathbf{X}}_0=0 \quad \bar{\mathbf{X}}_2-\bar{\mathbf{X}}_4=0 \end{aligned} \tag{10}$$

where the overbar “-” is used to identify different boundaries.

Putting Eqs. (9) and (10) together and writing the resulting linear algebraic equations in the form of matrix, we reach

$$\mathbf{KX}=\mathbf{F} \tag{11}$$

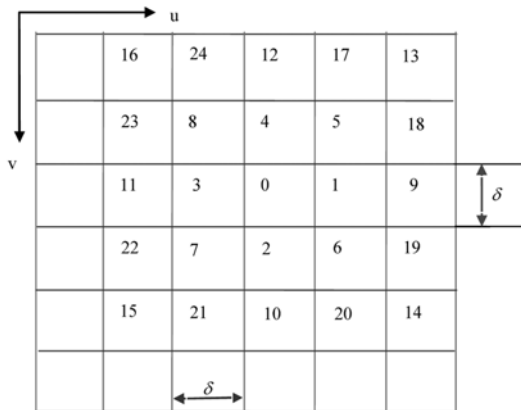


Fig. 3. Mesh of finite difference approximation.

Solving equation (11), we obtain the coordinate values of a surface at all nodes.

According to the principle of deformation equivalence, the deformation of curve i at parametric position $u = u_i$ should approximately be equal to that of the surface at the same position. The error function between them is

$$\mathbf{E}_i(v) = \frac{1}{EI_i\pi^4} \sum_{n=1}^{\bar{N}} \frac{\mathbf{p}_{in}}{n^3} \\ \left\{ \pi\{-1+[2+(-1)^n]v-[1+(-1)^n]v^2\}v+\frac{1}{n}\sin n\pi v \right\} - \mathbf{X}(u_i,v) \tag{12}$$

where $\mathbf{X}(u_i, v)$ represents the deformation of a surface at curve i which is determined by equation (11).

By minimizing the absolute error sum of equation (12), we obtain the equivalent force \mathbf{p}_i through \mathbf{p}_{in} in the equation. Then we substitute \mathbf{p}_i into equation (6) to determine the deformation of curve i .

Taking the deformation of a male chest to be an example, the deformation region is parameterized within $0 \leq u \leq 1$ and $0 \leq v \leq 1$. A concentrated force \mathbf{p}_0 is applied at $u_{p0} = v_{p0} = 0.5$ which causes the deformation of the male chest as indicated in Figure 4b where 4a is the original shape. With the above method, the concentrated force \mathbf{p}_i acting at the centre of each surface curve is determined. Finally, the deformation of the curve is calculated and the deformed shape of the male chest created from these deformed curves is depicted in Figure 4c.

Clearly, using the equivalent force determined by the above method gives a very good approximation of the deformed surface.

5. Mathematical model and determination of curve deformations

After changing the geometric properties and externally applied forces acting a surface into those acting the surface curves describing the surface, we can determine curve deformations with these quantities.

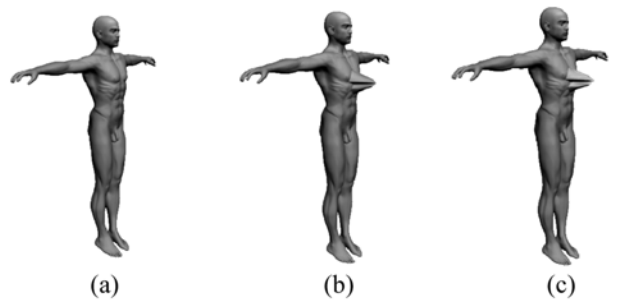


Fig. 4. Comparison between different surface manipulation approaches. (a) Original model, (b) Chest deformation by direct surface manipulation, (c) Chest deformation by curve-based surface manipulation.

As discussed above, bending deformation of a curve is similar to that of an elastic beam. Therefore, we can use the similar mathematical model of bending deformations of an elastic beam to describe the deformations of a curve which is a vector-valued fourth order ordinary differential equation in the form of

$$EI_i \frac{d^4 \mathbf{X}_i(v)}{dv^4} = \mathbf{q}_i \quad (13)$$

where \mathbf{X}_i is a vector-valued deformation function, I_i is the moment of inertia of surface curve i , and \mathbf{q}_i is a bending force acting on surface curve i .

In Section 4, we have presented the solution of equation (13) for the deformation region without coincidence boundaries. However, for character models, two boundaries in parametric direction v usually coincide. In order to develop an analytical solution of equation (13) for the modelling of virtual characters, we unify the mathematical description of concentrated and line distribution forces of surface curves with the following series

$$\mathbf{q}_i = \mathbf{c}_0 + \sum_{n=1}^N (\mathbf{c}_{2n-1} \sin 2n\pi v + \mathbf{c}_{2n} \cos 2n\pi v) \quad (14)$$

where \mathbf{c}_n ($n = 0, 1, 2, \dots, 2N$) are vector-valued unknown constants.

For a concentrated bending force \mathbf{Q}_i acting at position v_j of surface curve i , the unknown constants \mathbf{c}_n ($n = 0, 1, 2, \dots, 2N$) are given by the following equations

$$\begin{aligned} \mathbf{c}_0 &= \mathbf{Q}_i \\ \mathbf{c}_{2n-1} &= 2\mathbf{Q} \sin 2n\pi v_j \\ \mathbf{c}_{2n} &= 2\mathbf{Q} \cos 2n\pi v_j \\ (n &= 1, 2, \dots, N) \end{aligned} \quad (15)$$

For a uniformly distributed bending line force \mathbf{q}_i acting within $v_0 \leq v \leq v_1$ of surface curve i , the unknown constants \mathbf{c}_n ($n = 0, 1, 2, \dots, 2N$) are determined by the equations below

$$\begin{aligned} \mathbf{c}_0 &= (v_1 - v_0) \mathbf{q}_i \\ \mathbf{c}_{2n-1} &= \frac{\mathbf{q}_i}{n\pi} (\cos 2n\pi v_1 - \cos 2n\pi v_0) \\ \mathbf{c}_{2n} &= \frac{\mathbf{q}_i}{n\pi} (\sin 2n\pi v_1 - \sin 2n\pi v_0) \\ (n &= 1, 2, \dots, N) \end{aligned} \quad (16)$$

According to the mathematical representation for bending forces and ordinary differential equation (13), the deformation

of surface curve i can be described with the following function

$$\mathbf{X}_i = \sum_{j=0}^4 \mathbf{e}_j v^j + \sum_{n=1}^N (\mathbf{d}_{2n-1} \sin 2n\pi v + \mathbf{d}_{2n} \cos 2n\pi v) \quad (17)$$

where \mathbf{e}_j ($j = 0, 1, 2, \dots, 4$) and \mathbf{d}_n ($n = 1, 2, \dots, 2N$) are unknown constants.

Substituting equation (17) into (13), the unknown constants \mathbf{e}_4 and \mathbf{d}_n ($n = 1, 2, \dots, 2N$) are determined by

$$\begin{aligned} \mathbf{e}_4 &= \frac{\mathbf{c}_0}{24EI_i} \\ \mathbf{d}_{2n-1} &= \frac{\mathbf{c}_{2n-1}}{16\pi^4 n^4 EI_i} \\ \mathbf{d}_{2n} &= \frac{\mathbf{c}_{2n}}{16\pi^4 n^4 EI_i} \\ (n &= 1, 2, \dots, 2N) \end{aligned} \quad (18)$$

The remaining unknown constants \mathbf{e}_j ($j = 0, 1, 2, 3$) can be determined by the boundary constraints described below.

If the surface curve is closed, the same values of the position and first to second derivatives at $v = 0$ and $v = 1$ are required to maintain positional and high order continuities of surface curves at this position, i. e.,

$$\begin{aligned} \mathbf{X}_i(v=0) &= \mathbf{X}_i(v=1) \\ \frac{d^j \mathbf{X}_i(v=0)}{dv^j} &= \frac{d^j \mathbf{X}_i(v=1)}{dv^j} \\ (j &= 1, 2) \end{aligned} \quad (19)$$

Substituting equation (17) into (19), we find that \mathbf{e}_0 has no effect on boundary constraints (19). Therefore, we set $\mathbf{e}_0 = 0$, use equation (19) to determine the remaining unknown constants \mathbf{e}_j ($j = 1, 2, 3$), and write them in the following equation

$$\begin{aligned} \mathbf{e}_0 &= 0 \\ \mathbf{e}_1 &= 0 \\ \mathbf{e}_2 &= \frac{\mathbf{c}_0}{24EI_i} \\ \mathbf{e}_3 &= -\frac{\mathbf{c}_0}{12EI_i} \end{aligned} \quad (20)$$

For known surface curve i , we apply proper bending forces on it. With the bending forces and equation (17), we can calculate the bending deformations of the surface curve. After determining the bending deformations of all surface curves, the deformed surface curves are used to create the deformed shape of a surface and animate skin deformations.

We demonstrate how physical and geometric properties as well as externally applied forces influence surface deformation in Figures 5, 6 and 7, respectively.

First, how physical properties affect surface deformations is investigated. The deformation region for this example is taken to be the pig torso shown in Figure 5a which is defined with 9 closed surface curves.

From two boundary curves to the middle curve, Young's modulus is decreased to achieve different curve deformation. For each curve, Young's modulus drops against time. Figure 5b gives the obtained torso shape at the middle pose and Figure 5c presents the generated torso shape at the final pose. For the influence of Poisson's ratio, the original torso shape is same as that in Figure 5a. From two boundary curves to the middle curve, Poisson's ratio is increased. For each curve, Poisson's ratio rises with time. The created torso shapes at the middle pose and final pose are depicted in Figures 5d and 5e, respectively.

Next, the effect of geometric properties on surface deformations is examined. For this example, the neck of an arrui shown in Figure 6a is taken to be a deformation region and 8 closed curves are used to define the deformation region. The variations of the width and thickness of the surface are same as that of Young's modulus and Poisson's ratio, respectively. The width drops but the thickness rises from two boundary curves to the two middle curves. For each curve, the width decreases but the thickness increases against time. The obtained neck shapes at the middle and final poses caused by the change of the width are shown in Figures 6b and 6c and those caused by the change of the thickness are indicated in Figures 6d and 6e.

Finally, the influence of externally applied forces on surface deformations is shown in Figure 7. For this example, the deformation region is taken to be the trunk of an elephant which is described with 21 closed surface

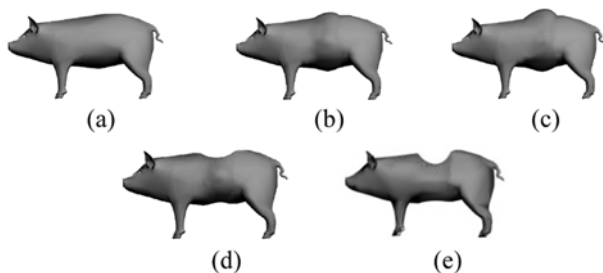


Fig. 5. Effects of physical properties on the skin deformation. (a) Original model, (b) and (c) Torso shape at middle and final poses caused by the change of Young's modulus, (d) and (e) Torso shape at middle and final poses caused by the change of Poisson's ratio.

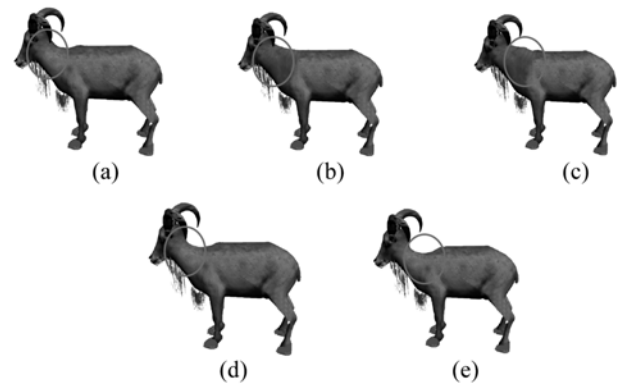


Fig. 6. Effects of geometric properties on the skin deformation. (a) Original model, (b) and (c) Neck shape at middle and final poses caused by the change of the width, (d) and (e) Neck shape at middle and final poses caused by the change of the thickness.

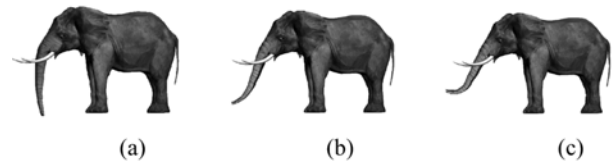


Fig. 7. Effects of externally applied forces on the skin deformation. (a) Undeformed trunk at the initial pose, (b) Deformed trunk at the middle pose, (c) Deformed trunk at the final pose.

curves. Different forces are applied on different curves to change the trunk shape in Figure 7a into that in Figures 7b and 7c, respectively.

6. Application examples

In this section, we give two examples to demonstrate the applications of our proposed method in skin deformation.

The first example is to animate the model of a horse leg. Two example skin shapes indicated in Figures 8a and 8e are known. They are inserted into equation (17). After considering equations (18) and (20), we obtain the force fields of these two example skin shapes and use them and equation (17) to create in-between skin shapes depicted in Figure 8b to Figure 8d.

The second example is to animate a human arm model. The arm model indicated in Figure 9b is described with the surface curves given in Figure 9a. For this example, we use the skin shape at 3 different poses: an initial pose in Figure 9b, a middle pose in Figure 9e, and a final pose in Figure 9h.

Using the skin at these three poses as example shapes, we achieve the shapes between these example skin shapes. The images in Figures 9c, 9d, 9f and 9g are the skin deformations obtained from our proposed method.

7. Conclusions

By introducing a curve based surface manipulation method combined with the physics and example based

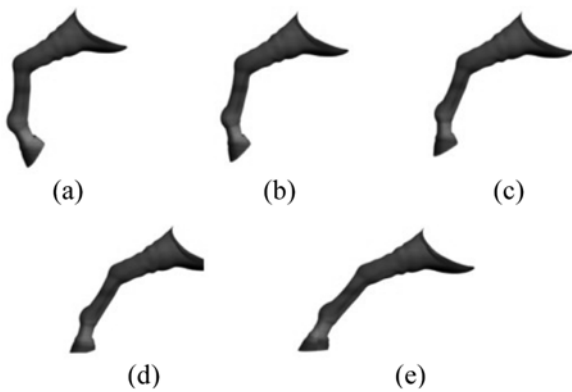


Fig. 8. Animation of a horse leg.

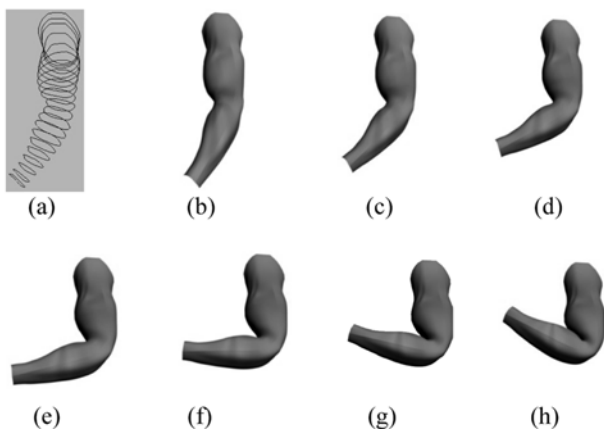


Fig. 9. Animation of a human arm.

approach and considering the equivalence principles of physical properties, geometric properties and externally applied forces between a surface and the corresponding curves, in this paper we have presented a simple and efficient method to animate skin deformations.

To represent a surface with curves reduces a typical 2D problem into a 1D problem, making it much less computation-intensive. A key step to maintain the quality however is to ensure the representation to have equivalent geometric and physical properties associated with the surfaces. This is tricky, especially we also use externally added virtual forces as a shape manipulation tool. We have employed a fourth order ordinary differential equation to code the physical behaviour into the curves. Using a small number of examples, we have demonstrated with examples that the conversion has not arrived at the price of quality. To produce the inbetween deformations, we only require two example skin shapes and the surface curves are deformed effectively.

8. Acknowledgements

We are grateful to Autodesk for their donation of the Maya software licenses. Some mesh data used in this project was made available by '500 3D-Objects' ([http://](http://www.taschen.com)

www.taschen.com) and Robert Sumner and Jovan Popovi from the Computer Graphics Group at MIT.

References

- [1] You, L.H., Chaudhry, E., You, X.Y. and Zhang, Jian J. (2009), Physics and example based skin deformations for character animation, In Proceedings of 11th IEEE International Conference on Computer-Aided Design and Computer Graphics, IEEE Press, 62-67.
- [2] Thalmann, N.M., Laperrière, R. and Thalmann, D. (1988), Joint-dependent local deformations for hand animation and object grasping, In Proceedings of Graphics interface, 26-33.
- [3] Lander, J. (May 1998), Skin them bones: Game programming for the web generation, *Game Developer Magazine*, 11-16.
- [4] Lander, J. (October 1999), Over my dead, polygonal body, *Game Developer Magazine*, 11-16.
- [5] Weber, J. (2000), Run-time skin deformation, In Proceedings of Game Developers Conference.
- [6] Wang, X.C. and Phillips, C. (2002), Multi-weight enveloping: least-squares approximation techniques for skin animation, In Proceedings of 2002 ACM SIGGRAPH/EUROGRAPHICS symposium on Computer animation, ACM Press, 129-138.
- [7] Mohr, A. and Gleicher, M. (2003), Building efficient, accurate character skins from examples, *ACM Transactions on Graphics* 22(3), 562-568.
- [8] Kavan, L. and Žára, J. (2005), Spherical blend skinning: A real-time deformation of articulated models, In Proceedings of the 2005 Symposium on Interactive 3D Graphics and Games, 9-15.
- [9] Yang, X.S., Somasekharan, A. and Zhang, J.J. (2006), Curve skeleton skinning for human and creature characters, *Computer Animation and Virtual Worlds* 17, 281-292.
- [10] Lewis, L.P., Corder, M. and Fong, N. (2000), Pose space deformation: a unified approach to shape interpolation and skeleton-driven deformation, In Proceedings of the 27th annual conference on Computer graphics and interactive techniques, ACM Press/Addison-Wesley Publishing Co., 165-172.
- [11] Rhee, T., Lewis, J.P. and Neumann, U. (2006), Real-time weighted pose-space deformation on the GPU, *Computer Graphics Forum* 25(3), 439-448.
- [12] Mohr, A. and Gleicher, M. (2003), Building efficient, accurate character skins from examples, *ACM Transactions on Graphics (SIGGRAPH 03)* 22(3), 562-568.
- [13] Allen, B., Curless, B. and Popovi, Z. (2002), Articulated body deformation from range scan data, In Proceedings of the 2002 Conference on Computer Graphics (SIGGRAPH 02), ACM Press, 612-619.
- [14] Kurihara, T. and Miyata, N. (2004), Modeling deformable human hands from medical images, In Proceedings of the 2004 ACM SIGGRAPH/Eurographics symposium on Computer animation, Eurographics Association, 355-363.
- [15] Weber, O., Sorkine, O., Lipman, Y. and Gotsman, C. (2007), Context-aware skeletal shape deformation, *Computer Graphics Forum* 26(3), 265-274.
- [16] Scheepers, F.R., Parent, E., Carlson, W.E. and May, S.F. (1997), Anatomy-based modelling of the human musculature, In Proceedings of the 24th Annual Conference on Computer Graphics and Interactive Techniques (SIGGRAPH 97), ACM Press/Addison-Wesley Publishing Co., 163-172.
- [17] Jane, W. and Allen, V.G. (1997), Anatomically based modelling, In Proceedings of the 1997 Conference on

- Computer Graphics and Interactive Techniques (SIGGRAPH 97), ACM Press, 173-180.
- [18] Nedel, L. and Thalmann, D. (1998), Modeling and deformation of human body using an anatomically-based approach, In Proceedings of the Computer Animation, IEEE Computer Society, 34-40.
- [19] Nedel, L. and Thalmann, D. (2000), Anatomic modelling of deformable human bodies, *The Visual Computer* 16, 306-321.
- [20] Aubel, A. and Thalmann, D. (2001), Interactive modelling of the human musculature, In Proceedings of Computer Animation, Institute of Electrical and Electronics Engineers Inc., 167-173.
- [21] Maryann, S., Jane, W., Allen, V.G. (2002), Model-based reconstruction for creature animation, In Conference Proceedings on ASM SIGGRAPH Symposium on Computer Animation, Institute of Electrical and Electronics Engineers Inc., 139-146.
- [22] Guo, Z. and Wong, K.C. (2005), Skinning with deformable chunks, *Computer Graphics Forum (EUROGRAPHICS 05)* 24(3), 373-381.
- [23] Venkataraman, K., Lodha, S. and Raghavan, R. (2005), A kinematic-variational model for animating skin with wrinkles, *Computers & Graphics* 29, 756-770.
- [24] Yang, X.S. and Zhang, J.J. (2006), Automatic muscle generation for character skin deformation, *Computer Animation and Virtual Worlds* 17, 293-303.
- [25] You, L.H., Yang X.S. and Zhang, J.J. (2008), Dynamic skin deformation with characteristic curves, *Computer Animation and Virtual Worlds* 19(3-4), 433-444.
- [26] Shen, J., Thalmann, N. M. and Thalmann, D. (1994), Human skin deformation from cross sections, In Proceedings of Computer Graphics International, Melbourne, Australia.
- [27] Pyun, H., Shin, H.J. and Shin, S.Y. (2004), On extracting the wire curves from multiple face models for facial animation, *Computers & Graphics* 28 (5), 757-765.
- [28] Hyun, D.E., Yoon, S.H., Chang, J.W., Kim, M.S. and Jüttler, B. (2005), Sweep-based human deformation, *The Visual Computer* 21, 542-550.
- [29] Yoon, S.H. and Kim, M.S. (2006), Sweep-based freeform deformations, *Computer Graphics Forum* 25(3), 487-496.
- [30] Jha, K. (2008), Construction of branching surface from 2-D contours, *International Journal of CAD/CAM* 8(1), 21-28.
- [31] You, L.H., Rodriguez, J.R. and Zhang, J.J. (2006), Manipulation of Elastically Deformable Surfaces through Maya Plug-in, In Proceedings of International Conference on Geometric Modeling & Imaging, IEEE Computer Society, 15-21.

Dr. L. H. You is currently a senior research lecturer at the National Centre for Computer Animation, Bournemouth Media School, Bournemouth University, UK. His research interests are in computer graphics, computer animation, and geometric modelling.

X. Y. You is currently a part-time MSc student with Coventry University, UK. He was awarded a BSc degree in computer science by the University of Warwick, UK. He is interested in the research into computer graphics etc.

Ehtzaz Chaudhry is PhD student in the National Centre for Computer Animation, Bournemouth Media School, Bournemouth University, UK. He was awarded a BSc and an MSc degree in computer science. He received his second MSc degree in Computer Game Graphics & Animation from University of Westminster, UK. He has experience in C#, C++, Cuda, GPU and Maya plug-in programming. His research interests include Computer graphics, Computer animation, Skin deformation, GPU and Games.

Jian J. Zhang is Professor of Computer Graphics at the National Centre for Computer Animation and Director of Computer Animation Research Centre, Bournemouth Media School, Bournemouth University. His research interests include computer graphics, computer animation, physically-based simulation, geometric modeling, medical simulation and visualisation.



Dr. L. H. You



X. Y. You



Ehtzaz Chaudhry



Jian J. Zhang